

# Anisotropic Growth of TiO<sub>2</sub> onto Gold Nanorods for Plasmon-Enhanced Hydrogen Production from Water Reduction

Binghui Wu,<sup>†,‡,§</sup> Deyu Liu,<sup>†,§</sup> Syed Mubeen,<sup>†,#</sup> Tracy T Chuong,<sup>†</sup> Martin Moskovits,<sup>†</sup> and Galen D. Stucky<sup>\*,†,‡</sup>

<sup>†</sup>Department of Chemistry & Biochemistry, University of California, Santa Barbara, California 93106, United States

<sup>‡</sup>Collaborative Innovation Center of Chemistry for Energy Materials, Xiamen University, Xiamen 361005, China

## Supporting Information

**ABSTRACT:** Plasmonic metal/semiconductor heterostructures show promise for visible-light-driven photocatalysis. Gold nanorods (AuNRs) semi-coated with TiO<sub>2</sub> are expected to be ideally structured systems for hydrogen evolution. Synthesizing such structures by wet-chemistry methods, however, has proved challenging. Here we report the bottom-up synthesis of AuNR/TiO<sub>2</sub> nanodumbbells (NDs) with spatially separated Au/TiO<sub>2</sub> regions, whose structures are governed by the NRs' diameter, and the higher curvature and lower density of C<sub>n</sub>TAB surfactant at the NRs' tips than on their lateral surfaces, as well as the morphology's dependence on concentration, and alkyl chain length of C<sub>n</sub>TAB. The NDs show plasmon-enhanced H<sub>2</sub> evolution under visible and near-infrared light.

Photocatalysis has received significant attention for solar conversion to electricity or fuels based on electron/hole pair production in semiconductors.<sup>1</sup> However, this process is constrained mainly by low photocatalytic efficiency and limited visible and near-infrared (NIR) photoabsorption. Efficient engineering of the photocatalyst surface and interface is crucial to overcome these limitations.<sup>2</sup> Recently, surface plasmon resonance (SPR) of Au,<sup>2a,b,3</sup> Ag,<sup>4</sup> and Pd<sup>5</sup> nanoparticles (NPs) has been applied to efficiently enhance visible and NIR absorption and generate SPR hot electrons.<sup>2c,6</sup>

Among these nanostructures, gold nanorods (AuNRs) with tunable SPR are of particular interest for their wide range of light harvesting; panchromatic absorption toward the solar spectrum can significantly improve the solar energy conversion efficiency.<sup>3f</sup> Moreover, AuNRs are usually interfaced with efficient electron acceptors (e.g., TiO<sub>2</sub>,<sup>7</sup> graphene,<sup>8</sup> Pt<sup>3d</sup>) to maximize the charge separation of hot electrons. Recently, we developed an autonomous, AuNR/TiO<sub>2</sub>-based photocatalytic device with oxidation and reduction co-catalysts using nanofabrication techniques.<sup>2b</sup> We clearly demonstrated that the plasmonic metal/semiconductor interface—a Schottky junction—can effectively select out the hot electrons, so that all charge carriers involved in the oxidation and reduction steps arise from these hot electrons, which are generated by exciting surface plasmons in the nanostructured AuNRs. To recycle the photoreduction/-oxidation, extraction of the hot electrons requires both refilling of these electrons and an electron donor accessible region on the SPR metal surface.<sup>2b,3e,f,5b,6b,9</sup> The spatial separation structure (rather than homogeneous core/shell structure) can be provided

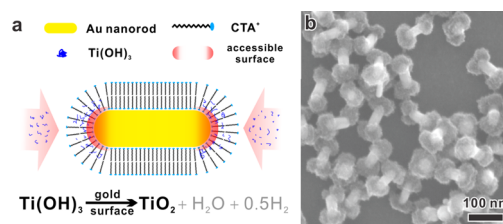


**Figure 1.** (a) Schematic showing the origin of anisotropic TiO<sub>2</sub> coating. (b) SEM image of the as-prepared AuNR/TiO<sub>2</sub> nanodumbbells. Synthetic conditions: 32 nm AuNRs (in diameter), 13.9 mM C<sub>16</sub>TAB.

by line-of-sight depositions using nanofabrication techniques that rely on advanced facilities and sophisticated operators. This nanofabrication method is usually not applicable for freestanding AuNRs synthesized by wet chemistry when there is no control of the orientation needed to create anisotropic AuNR/TiO<sub>2</sub> structures. Additionally, all wet-chemistry routes to such a well-defined spatial separation structure are challenging.

Anisotropic growth of TiO<sub>2</sub> onto AuNRs, instead of depositing AuNRs onto TiO<sub>2</sub>,<sup>10</sup> could give better contact between Au and TiO<sub>2</sub>. Because bilayers of surface-capping agents like cetyltrimethylammonium bromide (C<sub>16</sub>TAB) are more densely packed on AuNR sides than at the tips, this phenomenon has been utilized for the anisotropic overgrowth on C<sub>16</sub>TAB-capped AuNRs with metal heterostructures or silica.<sup>3b,d,11</sup> However, anisotropic overgrowth of semiconductors like TiO<sub>2</sub> on C<sub>16</sub>TAB-capped AuNRs in solution has been rarely reported.<sup>12</sup>

In this study, we report a wet-chemistry method for the anisotropic overgrowth of TiO<sub>2</sub> on AuNRs by using C<sub>n</sub>TAB as a soft template and by controlling the degree of hydrolysis of TiCl<sub>3</sub>. The roles of concentration and alkyl chain length of C<sub>n</sub>TAB as well as the diameter of the AuNRs were carefully studied. The as-prepared TiO<sub>2</sub>-tipped AuNRs have a dumbbell and spatial separation structure, and TiO<sub>2</sub> acts as a filter for hot electrons from AuNRs. This structure satisfies the electron refilling requirement and exhibits plasmon-enhanced hydrogen production from water reduction under visible and NIR light irradiation.

Figure 1a illustrates the formation of the dumbbell NPs by our bottom-up wet-chemistry method. The C<sub>n</sub>TAB bilayer confines the AuNR with only the tips accessible to Ti species. By controlling the hydrolysis of TiCl<sub>3</sub> via the pH or the reaction

Received: October 29, 2015

Published: January 25, 2016

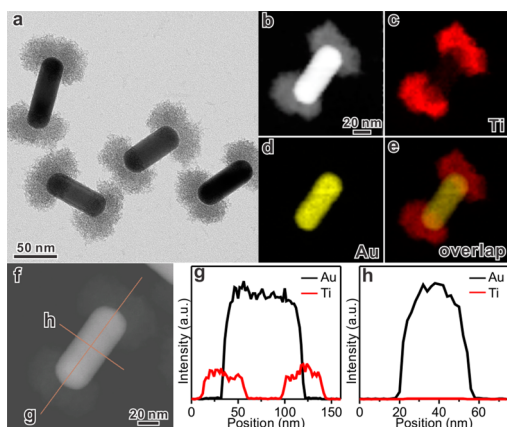


**Figure 2.** (a) TEM image, (b–e) HAADF-STEM image and elemental maps, and (f–h) elemental profiles of AuNR/TiO<sub>2</sub> NDs.

solution with NaHCO<sub>3</sub>,<sup>13a,b</sup> Ti<sup>3+</sup> is catalytically oxidized on the Au tips to form TiO<sub>2</sub>. Figure 1b is a typical SEM image of as-prepared AuNR/TiO<sub>2</sub> NDs using C<sub>16</sub>TAB-capped AuNRs as seeds (Figure S1). The product consists of uniform ND structures with the two tips of all the AuNRs coated with TiO<sub>2</sub> caps and the sides exposed. During the coating process, red shifts of SPR bands are observed *in situ* in the UV/vis spectra (Figure S2). This phenomenon corresponds to a local refractive index change due to the formation of the TiO<sub>2</sub> caps on the AuNR, and agrees with previous reports of dielectric material coatings on AuNPs.<sup>13b–d</sup> Due to the release of acid during the TiCl<sub>3</sub> hydrolysis, and the spatial coverage of the Au surface by the TiO<sub>2</sub> deposition, the reaction slows after ~30 min. In the synthesis, the spatial selectivity of the TiO<sub>2</sub> deposition on the AuNRs is controlled by engineering their surface chemistry. Another type of NPs, with a fully coated core/shell structure, can be prepared using a similar TiCl<sub>3</sub> hydrolysis process with the AuNRs pre-modified by an anionic surfactant, sodium dodecyl sulfate (SDS, Figure S3).

The anisotropic overgrowth of TiO<sub>2</sub> on AuNRs is further shown by TEM and HAADF-STEM-EDX analyses (Figures 2 and S4). These analyses reveal that the two caps are made from porous TiO<sub>2</sub> with basic building blocks <2 nm. The signal distribution obtained by linear scanning in the longitudinal direction clearly indicates the existence of two symmetrical TiO<sub>2</sub> caps. No Ti signal has been found by transverse scanning through the lateral side, further confirming specific tip-side selectivity of the deposition. Additionally, the significant distribution difference and shape of the caps suggest that the anisotropic deposition of TiO<sub>2</sub> is initiated from two tips of each AuNR and then extended toward the middle side surface of AuNRs. Note that the TiO<sub>2</sub> caps are amorphous based on the TiO<sub>2</sub> ultrafine domain size revealed in the HRTEM and XRD patterns (Figure S5).

Anisotropic overgrowth of TiO<sub>2</sub> on the AuNR tips can be explained by the bilayer adsorption structure of C<sub>16</sub>TAB and the special structure of the AuNR tips. The bilayer can behave as a soft template that guides the preferential bonding of the Au surface to solution species. Due to the curvature difference, the assembly of C<sub>16</sub>TAB on both tips of AuNR is less compact than that on the side.<sup>11,14</sup> The lower obstruction in these regions allows solution species to approach the AuNR tip surface (Figure 1a). This phenomenon has been previously used for the selective surface functionalization of AuNR tips.<sup>15</sup> By generalizing the side/tip-selective functionalization for hydrolysis reactions,

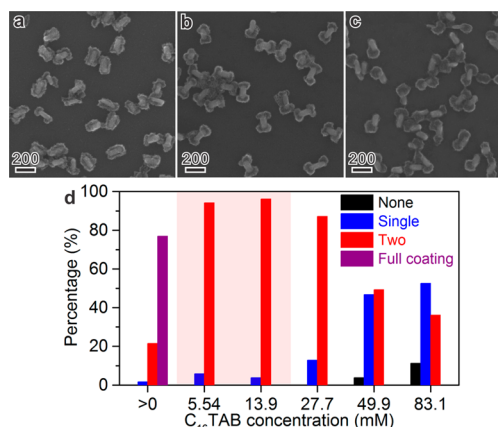


**Figure 3.** C<sub>16</sub>TAB concentration effect in TiO<sub>2</sub> growth on AuNRs. The same AuNR diameter (32 nm), but different C<sub>16</sub>TAB concentrations: (a) no additional C<sub>16</sub>TAB, (b) 5.54 mM, and (c) 83.1 mM. (d) The percentage histogram of coated AuNR tips. Note that the pink shadow indicates the C<sub>16</sub>TAB concentration between its first and second CMC.

Wang's group successfully prepared AuNRs with an anisotropic SiO<sub>2</sub> or Ag<sub>2</sub>O coating.<sup>11,16</sup> Similarly, here the TiO<sub>2</sub> formation process (a H<sub>2</sub> evolution reaction due to the oxidation of the TiCl<sub>3</sub> precursor<sup>13a</sup>) can be selectively catalyzed by the accessible AuNR tips, resulting in the spatially selective coating of TiO<sub>2</sub> on AuNRs. The anisotropic overgrowth can be due to both less dense assembly of C<sub>16</sub>TAB and herein less electrostatic repulsion between Ti species and the positively charged C<sub>16</sub>TAB bilayer.<sup>15c,17</sup> In contrast, SDS or similar surfactants modified AuNRs have a more random molecular assembly on them, resulting in homogeneous overgrowth of TiO<sub>2</sub> on AuNRs.<sup>13b,15c</sup>

To better understand why C<sub>16</sub>TAB promoted the anisotropic growth of TiO<sub>2</sub>, the relation between the growth and the concentration of C<sub>16</sub>TAB was studied. Figures 3 and S6 show the C<sub>16</sub>TAB concentration effect on TiO<sub>2</sub> growth using the same AuNRs of 32 nm in diameter. To reach >90% yield of AuNR-dumbbells, the C<sub>16</sub>TAB concentration must be appropriate, i.e., in the range between its first critical micelle concentration (CMC, 0.89 mM) and its second CMC (20 mM).<sup>18</sup> When C<sub>16</sub>TAB concentration is lower than the first CMC, most of the AuNRs are fully covered with a rough TiO<sub>2</sub> shell, due to the unstable and easily disrupted C<sub>16</sub>TAB bilayer.<sup>15c</sup> When the C<sub>16</sub>TAB concentration is greater than the second CMC, a large portion of the product has only one tip coated with TiO<sub>2</sub>, or is not coated at all, due to the ultra-dense bilayer of C<sub>16</sub>TAB. However, for concentrations of C<sub>16</sub>TAB between the first and second CMCs, the deposition of TiO<sub>2</sub> is effectively limited to two tips with a high yield. A similar result was reported by Wang et al.,<sup>11</sup> i.e., an appropriate C<sub>16</sub>TAB concentration (~6 mM) leads to effective overgrowth of SiO<sub>2</sub> onto AuNR tips. These results show that a well-assembled C<sub>16</sub>TAB bilayer is critical for the anisotropic overgrowth of TiO<sub>2</sub> on AuNRs.

Based on the assumption of the relationship between the selective coating and the C<sub>16</sub>TAB bilayer, curvatures of the AuNR tips should play a critical role. AuNRs with different diameters as the seeds were used in the presence of the same C<sub>16</sub>TAB concentration. The histogram in Figure 4a shows a correlation of AuNR diameters and the percentage of coated tips in the products. The trend shows that the thinner AuNRs, the harder it is to coat TiO<sub>2</sub> on the tips of the AuNRs (regardless of their lengths). A large percentage of the products formed using narrow AuNRs (diameter <20 nm) are either coated on a single tip or

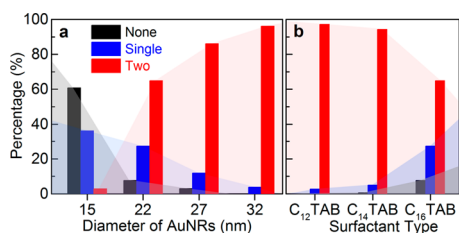


**Figure 4.** Percentage histogram of coated tips on AuNR/TiO<sub>2</sub> product synthesized under similar conditions, with (a) the same concentration of C<sub>16</sub>TAB (13.9 mM), but different AuNR diameters, and (b) the same AuNR diameter (22 nm), but different C<sub>n</sub>TABs (13.9 mM).

completely without coating (Figure S7). Since the curvature has a reciprocal relationship with the diameter, seemingly the C<sub>16</sub>TAB bilayer on thinner AuNRs should have a more open structure on the tips, which should allow the region to be coated more easily. On the other hand, the area on the tip of a thinner AuNR is also significantly reduced, thereby reducing the ability of nucleating TiO<sub>2</sub> caps and their stability on AuNR tips (see Note 1, page S3, for further discussion).

Since C<sub>16</sub>TAB cannot lead to the coating of thin AuNRs (<27 nm in diameter) to give a high yield of TiO<sub>2</sub> overgrowth, other C<sub>n</sub>TABs with shorter alkyl chain were studied. Figures 4b and S8 show the result of coating TiO<sub>2</sub> onto thin AuNRs (22 nm in diameter) in the presence of single C<sub>n</sub>TAB ( $n = 12, 14, 16$ ; the same molar concentration optimized for C<sub>16</sub>TAB was used for all). The yield of tip-selective coating on thin AuNRs is significantly improved when using C<sub>14</sub>TAB or C<sub>12</sub>TAB instead of C<sub>16</sub>TAB. Their shorter hydrocarbon chains give a weaker hydrophobic interaction between molecules, so that better permit a bilayer adsorption structure on the thin AuNR tip surface. Especially on the tips of thin AuNRs, the C<sub>14</sub>TAB or C<sub>12</sub>TAB bilayer allows Ti(III) species access to the catalytic Au surface more easily despite the higher curvature, thereby making a thicker TiO<sub>2</sub> deposition possible and compensating the instability from the smaller area on the tips of thin AuNRs. Furthermore, AuNR diameter effect in the presence of C<sub>12</sub>TAB (13.9 mM; its first CMC is ~14 mM)<sup>19</sup> was studied (Figure S9). For 15 nm AuNRs, C<sub>12</sub>TAB leads to higher possibility of tipped TiO<sub>2</sub> coating than C<sub>16</sub>TAB, which is converse for the case of 32 nm AuNRs. Indeed, our studies reveal that an optimum combination of C<sub>n</sub>TAB with specific carbon chain length and AuNR diameter is essential to obtain a high-yield anisotropic overgrowth of TiO<sub>2</sub> onto AuNR tips. Previous investigations were conducted using C<sub>18</sub>TAB or C<sub>18</sub>TAC for the overgrowth of metal heterostructures or silica on AuNRs with limited diameters;<sup>3b,d,11</sup> here we focus on varying the C number in C<sub>n</sub>TAB to control the capping agent functionality in heterogeneous overgrowth processes of TiO<sub>2</sub> on AuNRs with various diameters.

It should be noted that mixing two C<sub>n</sub>TABs with different C number can change the growth behavior of TiO<sub>2</sub> on AuNRs when compared to growth using a single C<sub>n</sub>TAB. Figure S10 shows the product prepared in a mixed C<sub>12</sub>TAB/C<sub>16</sub>TAB (1:1) solution. In this case, TiO<sub>2</sub> is inclined to coat the sharp corners which connect the side and the endmost tips of AuNRs, rather than the whole tips as in the case of single C<sub>n</sub>TAB (Figures S7d and S9d). This is also attributed to the limitation from C<sub>n</sub>TAB bilayer structure. As a mixture of two C<sub>n</sub>TABs, the entropic force makes C<sub>16</sub>TAB with longer hydrocarbon chains go to the less curved surface and push the shorter C<sub>12</sub>TAB aside to corners. The higher percentage of shorter C<sub>12</sub>TAB on sharp corners significantly reduces the

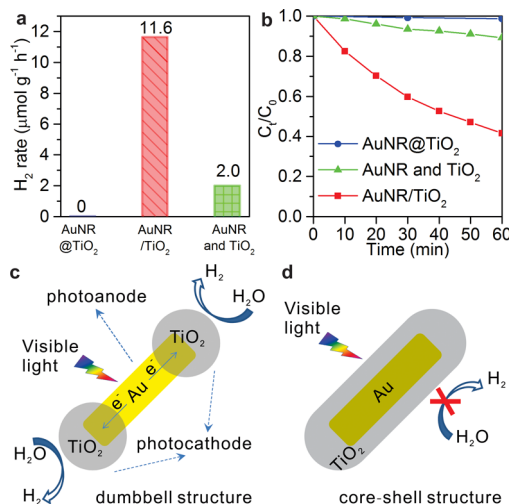


**Figure 5.** Comparison of (a) H<sub>2</sub> evolution rate by various catalysts, and (b) normalized concentration of MB vs irradiation time; both under visible illumination and in the presence of methanol and water. (c,d) Structure and mechanism of operation under visible light of (c) an individual AuNR/TiO<sub>2</sub> dumbbell and (d) core/shell AuNR@TiO<sub>2</sub>. In (c), hot electrons generated from plasmonic AuNRs are filtered out by the Au/TiO<sub>2</sub> Schottky barrier for photoreduction and regenerated from the electron donor (methanol here).

hindrance for TiO<sub>2</sub> deposition on that focused region and allows it to form small caps on the AuNR tips.

The most exciting feature of the designed AuNR/TiO<sub>2</sub> NDs is their ability to promote SPR-induced hot-electron generation under visible and NIR light. While AuNR@TiO<sub>2</sub> core/shell NPs and pure amorphous TiO<sub>2</sub> show no activity for H<sub>2</sub> evolution, AuNR/TiO<sub>2</sub> NDs exhibit relatively high photoactivity, compared to physically mixed AuNRs and amorphous TiO<sub>2</sub> (Figure 5a; AuNR#5 with 32 nm diameter were used). Note that the difference in the photocatalytic activity of these three samples does not result from the surface area or the mass of TiO<sub>2</sub>, since amorphous TiO<sub>2</sub> itself does not absorb visible light and a significantly excess quantity of TiO<sub>2</sub> was used in the mechanical mixture of AuNRs and TiO<sub>2</sub>. The activity of AuNR/TiO<sub>2</sub> NDs is higher than that of spherical AuNPs deposited on crystalline TiO<sub>2</sub> under similar condition.<sup>20</sup> Further increasing the crystallinity of the TiO<sub>2</sub> and adding co-catalysts could enhance the visible light performance of our AuNR/TiO<sub>2</sub> NDs.<sup>2b</sup> These control experiments clearly demonstrate the importance of ND structure with intimate physical contact and strong plasmonic coupling for enhanced charge separation in the plasmon-enhanced photocatalysis. The difference of the photocatalytic activities under visible light for the AuNR/TiO<sub>2</sub> NDs and the AuNR@TiO<sub>2</sub> core/shell structure further suggests that the plasmon-enhanced photocatalysis mechanism is plasmonic hot electron transfer due to localized SPR of AuNRs (which is dependent on the configuration/architecture of metal/semiconductor heterojunction), rather than plasmon-induced resonance energy transfer (based on the inactivity of the core/shell structure).<sup>21</sup>

Hot electron generation was further demonstrated in the photoreduction of methylene blue (MB), a model acceptor molecule (Figure 5b). After 60 min of irradiation, the AuNR/TiO<sub>2</sub> NDs exhibited ~60% reduction of the MB dye. In the control experiments, physically mixed AuNRs and TiO<sub>2</sub> solution exhibited ~10% reduction of the MB, while AuNR@TiO<sub>2</sub> core/shell structure showed insignificant activity (<1%; part of the activity may come from photobleaching<sup>22</sup>). These experiments

on the photoreduction of MB demonstrate the importance of close contact and the anisotropic assembly of the AuNR and TiO<sub>2</sub> domains for effective visible light photocatalysis.

Previous studies indicate that the SPR-induced hot electrons can be filtered out from metal NPs with the positive charges left behind.<sup>2b,c,3f,6b,15c</sup> Note that neither TiO<sub>2</sub> alone nor pure AuNRs can produce H<sub>2</sub> under similar conditions. For the NDs, the oxidation pathway is on their side surface (Figure 5c), where the lateral side of AuNRs can be directly exposed to electron donors so that oxidation reactions can take place. With AuNR partially exposed in the ND structure, AuNRs generate a concentrated electromagnetic field that focuses energy flux around the semiconductor, and thus enhance hot-electron generation and photocatalytic activity.<sup>2b,3d,6b,23</sup> As pointed out by Yates,<sup>24</sup> hot electrons generated in AuNRs under visible light that overcome the Schottky barrier (due to band bending; see Note 2, page S5, for further discussion) are likely to flow from AuNRs to TiO<sub>2</sub> and be available for photoreduction with TiO<sub>2</sub> acting as the electron-transfer medium. The ND structure ideally exploits such charge exchange opportunities, carrying out reduction processes on the TiO<sub>2</sub> then restoring charge balance to the Au core through oxidation reactions that would occur on the bare portions of the AuNRs (Figure 5c). A fully coated AuNR is denied of the opportunity for establishing such a complete circuit that allows both electrons and holes to access their appropriate reaction partners, thereby blocking the continuous flow of the hot charge carriers resulting from the excitation of the SPR (Figure 5d). Thus, we ascribe the better SPR photocatalytic performance of the NDs to their ability to present appropriate and separate regions where the oxidation and reduction processes can take place, as opposed to the core/shell NPs without such separate regions.

In summary, an easy, bottom-up, wet-chemistry technique for the synthesis of anisotropic TiO<sub>2</sub> overgrowth on AuNRs has been developed using the selective spatial assembly of a C<sub>n</sub>TAB bilayer on AuNR surfaces and the hydrolysis of TiCl<sub>3</sub>. The concentration, alkyl chain length of C<sub>n</sub>TAB, and diameter of AuNRs are important to control the selective overgrowth. The as-prepared AuNR/TiO<sub>2</sub> NDs exhibit plasmon-enhanced H<sub>2</sub> evolution under visible/NIR light. The created AuNR/TiO<sub>2</sub> interface with the AuNR side exposed, as a Schottky junction, can filter out SPR hot electrons from the AuNRs. Engineering the structure, e.g., by loading co-catalysts, may further improve its activity for the plasmon-induced H<sub>2</sub> evolution. This work shows an alternative solution of anisotropic TiO<sub>2</sub> overgrowth rather than nanofabrication techniques, and is expected to be a promising platform for the development of free-standing functional photocatalysts.

## ■ ASSOCIATED CONTENT

### 📄 Supporting Information

The Supporting Information is available free of charge on the ACS Publications website at DOI: 10.1021/jacs.5b11341.

Experimental details, microscopy images, XRD, and UV/vis spectra, including Table S1 and Figures S1–S10 (PDF)

## ■ AUTHOR INFORMATION

### Corresponding Author

\*stucky@chem.ucsb.edu

### Present Address

#S.M.: Department of Chemical and Biochemical Engineering, University of Iowa, Iowa City, IA 52242, USA

## Author Contributions

§B.W. and D.L. contributed equally.

## Notes

The authors declare no competing financial interest.

## ■ ACKNOWLEDGMENTS

This research was supported by the Center for Energy Efficient Materials, an Energy Frontier Research Center funded by the U.S. Department of Energy, Office of Science, Basic Energy Sciences, under award no. DE-SC0001009, and by the National Science Foundation (DMR 0805148). The MRL Shared Experimental Facilities are supported by the MRSEC Program of the NSF under Award No. DMR 1121053. B.W. was partially supported by China Scholarships Council for this research. We gratefully acknowledge Jialuo Li (TAMU) for help with drawing the table of contents graphic.

## ■ REFERENCES

- (1) Ma, Y.; et al. *Chem. Rev.* **2014**, *114*, 9987.
- (2) (a) Tada, H.; et al. *Nat. Mater.* **2006**, *5*, 782. (b) Mubeen, S.; et al. *Nat. Nanotechnol.* **2013**, *8*, 247. (c) Kochuveedu, S. T.; et al. *Chem. Rev.* **2013**, *42*, 8467. (d) Liu, C.; et al. *Nano Lett.* **2013**, *13*, 2989.
- (3) (a) Tian, Y.; Tatsuma, T. *J. Am. Chem. Soc.* **2005**, *127*, 7632. (b) Wang, F. *J. Am. Chem. Soc.* **2013**, *135*, 5588. (c) Wu, K. F.; et al. *Nano Lett.* **2013**, *13*, 5255. (d) Zheng, Z. K.; Tachikawa, T.; Majima, T. *J. Am. Chem. Soc.* **2014**, *136*, 6870. (e) Moskovits, M. *Nat. Nanotechnol.* **2015**, *10*, 6. (f) Mubeen, S.; et al. *Nano Lett.* **2015**, *15*, 2132.
- (4) (a) Christopher, P.; Xin, H. L.; Linic, S. *Nat. Chem.* **2011**, *3*, 467. (b) Li, G.; et al. *Nano Lett.* **2015**, *15*, 3465. (c) Ingram, D. B.; Linic, S. *J. Am. Chem. Soc.* **2011**, *133*, 5202.
- (5) (a) Long, R.; et al. *Angew. Chem., Int. Ed.* **2014**, *53*, 3205. (b) Long, R.; et al. *Angew. Chem., Int. Ed.* **2015**, *54*, 2425.
- (6) (a) Jiang, R.; et al. *Adv. Mater.* **2014**, *26*, 5274. (b) Clavero, C. *Nat. Photonics* **2014**, *8*, 95.
- (7) Pu, Y. C.; et al. *Nano Lett.* **2013**, *13*, 3817.
- (8) Hoggard, A.; et al. *ACS Nano* **2013**, *7*, 11209.
- (9) (a) Furube, A.; et al. *J. Am. Chem. Soc.* **2007**, *129*, 14852. (b) Wang, C.; Astruc, D. *Chem. Soc. Rev.* **2014**, *43*, 7188. (c) DuChene, J. S.; et al. *Angew. Chem., Int. Ed.* **2014**, *53*, 7887.
- (10) Liu, L. Q.; et al. *Angew. Chem., Int. Ed.* **2013**, *52*, 6689.
- (11) Wang, F.; et al. *Angew. Chem., Int. Ed.* **2013**, *52*, 10344.
- (12) Seh, Z. W.; et al. *Angew. Chem., Int. Ed.* **2011**, *50*, 10140.
- (13) (a) Liu, R.; Sen, A. *J. Am. Chem. Soc.* **2012**, *134*, 17505. (b) Fang, C. H.; et al. *Energy Environ. Sci.* **2014**, *7*, 3431. (c) Chen, H. J.; et al. *ACS Nano* **2012**, *6*, 7162. (d) Li, B. X.; et al. *ACS Nano* **2014**, *8*, 8152.
- (14) Zhang, S. Z.; et al. *Chem. Commun.* **2007**, 1816.
- (15) (a) Nie, Z. H.; et al. *Nat. Mater.* **2007**, *6*, 609. (b) Liu, K.; Zhao, N. N.; Kumacheva, E. *Chem. Soc. Rev.* **2011**, *40*, 656. (c) Chen, H.; et al. *Chem. Soc. Rev.* **2013**, *42*, 2679.
- (16) Bao, Z. H.; et al. *J. Mater. Chem.* **2011**, *21*, 11537.
- (17) (a) Perez-Juste, J.; et al. *Adv. Funct. Mater.* **2004**, *14*, 571. (b) Correa-Duarte, M. A.; et al. *Angew. Chem., Int. Ed.* **2005**, *44*, 4375.
- (18) Li, N. B.; Liu, S. P.; Luo, H. Q. *Anal. Lett.* **2002**, *35*, 1229.
- (19) Bahri, M. A.; et al. *Colloids Surf., A* **2006**, *290*, 206.
- (20) Ding, D.; et al. *Nano Lett.* **2014**, *14*, 6731.
- (21) (a) Cushing, S. K.; et al. *Phys. Chem. Chem. Phys.* **2015**, *17*, 30013. (b) Cushing, S. K.; et al. *J. Phys. Chem. C* **2015**, *119*, 16239.
- (22) Costi, R.; et al. *Nano Lett.* **2008**, *8*, 637.
- (23) (a) Cushing, S. K.; et al. *J. Am. Chem. Soc.* **2012**, *134*, 15033. (b) Hou, W. B.; et al. *ACS Catal.* **2011**, *1*, 929.
- (24) Zhang, Z.; Yates, J. T. *Chem. Rev.* **2012**, *112*, 5520.